

# An Enhanced MIMO Hardware Demonstrator - Polarization Diversity in Adaptive OFDM Systems

Mark Petermann\* , Markus Stefer\*\*, Dirk Wübben\* , Martin Schneider\*\*, Karl-Dirk Kammeyer\*

\*Department of Communications Engineering

Email: {petermann, wuebben, kammeyer}@ant.uni-bremen.de

\*\*RF & Microwave Engineering Laboratory

Email: {markus.stefer, martin.schneider}@hf.uni-bremen.de

University of Bremen, 28359 Bremen, Germany

**Abstract**—The performance of multiple-input multiple-output (MIMO) systems is affected by the spatial correlation properties, which depend on the array configuration and the channel characteristics. The configuration can be influenced by manipulating the radiation patterns of the antennas, the antenna spacing and the array geometry. To decrease the spatial correlation effects, e.g., the antenna spacing can be increased, which is usually undesirable in mobile devices. Here, the utilization of polarization diversity techniques comes into consideration. This paper deals with the application and comparison of different polarized transmit/receive array setups in indoor environments using a multiple antenna demonstrator in uncoded adaptive MIMO-OFDM scenarios. Measurement results indicate a decreased correlation of the spatial subchannels, a higher MIMO capacity for cross-polarized antenna arrays and lower bit error rates with bit and power loading algorithms.

## I. INTRODUCTION

Multiple-input multiple-output (MIMO) schemes became state-of-the-art when thinking about enhancing data rates and reliability in future mobile communications [1]. Generally, the intention is to provide either diversity or multiplexing principles in the system, both of which are affected by the spatial correlation properties, which depend on the array configuration and the mobile radio channel characteristics. The configuration can be influenced by tuning the radiation patterns of the antennas, changing the antenna spacing or the array geometry. To decrease the spatial correlation effects, e.g., the antenna spacing can be increased to enable space diversity. This is usually undesirable in mobile devices, where in practice small-scale components and low-complexity algorithms dominate the design process. The utilization of polarization diversity, where

the antennas are designed such that orthogonally polarized radiation characteristics are achieved, may be one solution to achieve similar results. It was shown that exploiting the vertical and the horizontal polarization lead to gains in the multiplexing case, where no gains are achieved when using diversity schemes [2]. The trade-off between correlation and diversity properties of the configuration is also discussed in [3].

Further results showed the potential of space savings with cross polarization discrimination (XPD) at both transceiver ends compared to conventional space diversity [4], also in the context of long term evolution (LTE) [5]. In LTE, the orthogonal frequency division multiplexing (OFDM) air interface technology is applied [6], which offers additional degrees of freedom concerning adaptive polarization on a subcarrier basis [7]. Problems about the significant mean signal power difference of unequally polarized branches and principles to overcome this by means of circular polarization are discussed, e.g., in [3], [8], but are beyond the scope of this contribution. In this paper, the application of different polarized transmit/receive array setups in indoor environments using a multiple antenna demonstrator [9] in uncoded adaptive MIMO-OFDM scenarios at 2.4 GHz is investigated. A comparison is made with respect to capacity and bit error rates.

The remainder of the paper is organized as follows. In Sec. II the system model and the applied antenna array setups are described. In addition, the considered eigenanalysis and the information theoretical backgrounds are introduced. Subsequently, the enhanced MIMO hardware demonstrator is presented in Sec. III. Measurement results for the estimated eigenvalue distribution of different polarizations and the resulting bit error rates in adaptive systems are shown in Sec. IV. Finally, a conclusion is given in Sec. V.

This work was supported in part by the German Research Foundation (DFG) under grant KA841-21/1 and SCHN1147/2-1.

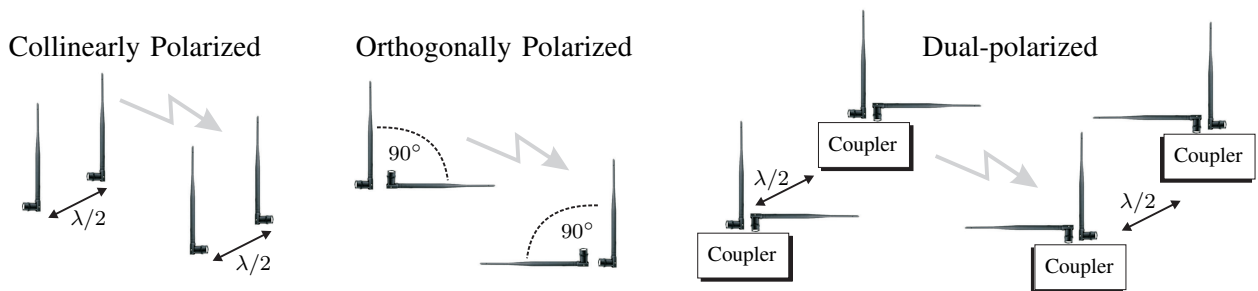


Fig. 1. Different applied antenna configurations of the MASI-2 system in the experimental investigations

## II. SYSTEM MODEL

### A. Polarized Arrays

Especially in small office room scenarios the need for efficient space exploitation in line-of-sight (LOS) conditions is existent. Due to the LOS component of the receive signal only one dominant eigenmode is apparent in several measurement campaigns. The idea of polarization diversity, where both the horizontal and vertical polarization of the antennas are utilized, is an attractive solution to achieve more robust systems [10].

In the following, this diversity principle is investigated with an antenna demonstrator, which is equipped with multiple dipoles with omnidirectional radiation patterns and a polarization along the antenna axis. Throughout the evaluation, different antenna configurations of the dipole elements are utilized, which are depicted in Fig. 1. The inter-element spacing for a standard collinearly polarized uniform linear array is  $0.5\lambda$ , where  $\lambda$  is the free space wavelength. For the array configuration utilizing two polarizations, named orthogonally polarized in the following, the second antenna is rotated by 90 degree and placed as close as possible to the antenna enabling the polarization plane perpendicular to that of the first antenna. The receive antenna is rotated accordingly to receive the same amount of energy and to fully enable the polarization diversity. A third configuration is the utilization of dual-polarized antennas. Therefore, two dipoles are connected via a coupler, consequently building one virtual dual-polarized antenna element. Again, the same receive array configuration is applied.

### B. Eigenanalysis and Capacity Considerations

The different array geometries as described in Sec. II-A shall be analyzed with respect to the eigenvalue distributions and ergodic capacity results. Therefore, a MIMO system with  $N_T$  transmit and

$N_R$  receive antennas is considered. The receive covariance matrix of the instantaneous channel matrix  $\mathbf{H}(t)$  at time instant  $t$  in each configuration is defined as

$$\Phi_{\mathbf{H}\mathbf{H}} = \mathbb{E}\left\{\mathbf{H}(t)\mathbf{H}(t)^H\right\} = \mathbf{H}\mathbf{H}^H = \mathbf{Q}\mathbf{\Lambda}\mathbf{Q}^H, \quad (1)$$

where time index  $t$  can be omitted due to the assumed static scenario. The diagonal matrix  $\mathbf{\Lambda} = \text{diag}\{\lambda_1, \dots, \lambda_{N_R}\}$  contains the eigenvalues and  $\mathbf{Q}$  the corresponding eigenvectors. Instead of calculating the eigendecomposition in (1), the singular value decomposition (SVD) can be used for the eigenanalysis such that

$$\mathbf{H}(t) = \mathbf{U}\mathbf{\Sigma}\mathbf{V}^H \quad (2)$$

holds. The diagonal matrix  $\mathbf{\Sigma} = \text{diag}\{\sigma_1, \dots, \sigma_r\}$  with  $\sigma_1 \geq \sigma_2 \geq \dots \geq \sigma_r \geq 0$  and  $\text{rank } r = \min\{N_R, N_T\}$  now comprises the singular values, which are related to the eigenvalues such that  $\lambda_i = \sigma_i^2$ . The evaluation in terms of the cumulative distribution function (CDF) shows the probability that the eigenvalue  $\lambda_i$  is lower or equal than a certain value  $\gamma$

$$\text{CDF}(\lambda_i) = \text{Pr}(\lambda_i \leq \gamma). \quad (3)$$

The analysis of the adaptive systems is conducted based on a single-user MIMO-OFDM system with  $N_C$  subcarriers using a bit and power loading algorithm as in [11]. For the sake of brevity, the subcarrier index for the considered OFDM system as in Sec. III-B is neglected here, as the results can be easily extended on a per subcarrier basis. The system equation for such a scheme using (2) reads as follows

$$\mathbf{y} = \mathbf{H}\mathbf{P}^{1/2}\mathbf{x} + \mathbf{n} = \mathbf{U}\mathbf{\Sigma}\mathbf{V}^H\mathbf{P}^{1/2}\mathbf{x} + \mathbf{n}, \quad (4)$$

with transmit data vector  $\mathbf{x} \in \mathbb{C}^{N_T}$ , receive data vector  $\mathbf{y} \in \mathbb{C}^{N_R}$ , noise term  $\mathbf{n} \sim \mathcal{N}_C(\mathbf{0}_{N_R}, \sigma_N^2 \mathbf{I}_{N_R})$  and the diagonal power allocation matrix  $\mathbf{P} = \text{diag}\{P_1, \dots, P_{N_T}\}$ . Using the

multiplications  $\tilde{\mathbf{y}} = \mathbf{U}^H \mathbf{y}$ ,  $\tilde{\mathbf{x}} = \mathbf{V}^H \mathbf{x}$  and  $\tilde{\mathbf{n}} = \mathbf{U}^H \mathbf{n}$  an equivalent system model is obtained

$$\tilde{\mathbf{y}} = \mathbf{P}^{1/2} \boldsymbol{\Sigma} \tilde{\mathbf{x}} + \tilde{\mathbf{n}}. \quad (5)$$

As  $\boldsymbol{\Sigma}$  is strictly diagonal,  $r = \min\{N_R, N_T\}$  decoupled parallel channels with different modulation and power according to [11] are existent. The corresponding ergodic capacity of (4) results from the maximization of the mutual information  $I(\mathbf{x}; \mathbf{y} | \mathbf{H})$  depending on the transmit covariance matrix  $\boldsymbol{\Phi}_{\mathbf{x}\mathbf{x}}$  such that

$$C = \mathbb{E} \left\{ \max_{\boldsymbol{\Phi}_{\mathbf{x}\mathbf{x}}} I(\mathbf{x}; \mathbf{y} | \mathbf{H}) \right\} \quad (6a)$$

$$= \mathbb{E} \left\{ \max_{\boldsymbol{\Phi}_{\mathbf{x}\mathbf{x}}} \text{ld} \left( \mathbf{I}_{N_R} + \frac{1}{\sigma_N^2} \mathbf{H} \boldsymbol{\Phi}_{\mathbf{x}\mathbf{x}} \mathbf{H}^H \right) \right\}, \quad (6b)$$

which can be decomposed to

$$C = \mathbb{E} \left\{ \sum_{i=1}^r \text{ld} \left( 1 + \frac{\lambda_i P_i}{\sigma_N^2} \right) \right\}. \quad (7)$$

Hence, (7) is the ergodic capacity of the investigated system, while  $\mathbb{E}\{\cdot\}$  denotes the expectation. In contrast to (5), the power  $P_i$  for the parallel channels is calculated according to the waterfilling principle to maximize (7) [12]

$$P_i = \left( \theta - \frac{1}{\lambda_i} \right)^+. \quad (8)$$

In (8),  $(x)^+ = \max\{x, 0\}$  holds, where  $\theta$  is the waterfilling level. The total power constraint

$$P = \text{tr}(\boldsymbol{\Phi}_{\mathbf{x}\mathbf{x}}) = \text{tr}(\mathbf{P}) = \sum_{i=1}^r P_i = \sum_{i=1}^r \left( \theta - \frac{1}{\lambda_i} \right)^+ \quad (9)$$

has to be set to investigate the capacities in different signal-to-noise regions.

### III. MULTIPLE ANTENNA SYSTEM FOR ISM-BAND TRANSMISSION

#### A. Measurement Setup

For the real system measurements an enhanced direct-conversion based multiple antenna system called Multiple Antenna System for ISM-Band Transmission version 2 (MASI-2) firstly applied in [9] is used. This demonstrator provides a verification method of comparing simulation results with a real transmission considering general impairments like synchronization and timing aspects. In the MASI-2 system the Tx/Rx chains are connected to a single-pole-double-throw (SPDT) switch, which allows for time duplex switching. Each Tx/Rx chain has its own front-end due to a modular

architecture. Now, a  $2 \times 2$  transceiver system with antenna spacing  $\lambda/2$  is available that can be used to investigate adaptive MIMO schemes in time division duplex (TDD) mode. The carrier frequency of the system is fixed to  $f_{\text{LO}} = 2.44$  GHz here, where the LO signals are provided by two external signal generators to ensure very small frequency offsets. The sampling rate is  $f_s = 50$  MHz and an oversampling factor of 8 is used. Three different scenarios are investigated throughout this work. The first and initial measurements were conducted in an anechoic chamber with an array separation of around 3 m, with Fig. 2 showing an exemplary setup in the measurement series. The second measurement

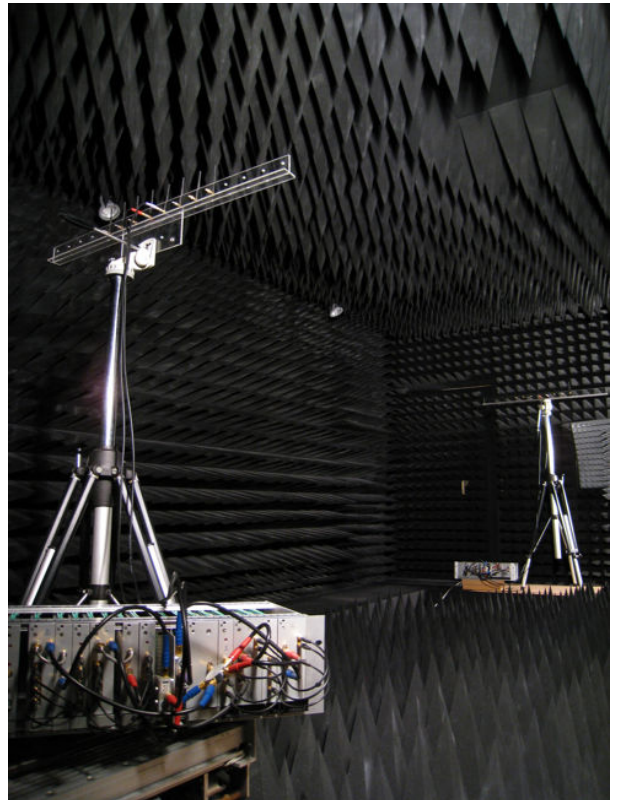


Fig. 2. MASI-2 system setup with collinearly polarized antennas in an anechoic chamber

setup is a LOS office room scenario, where again the antenna arrays are separated by a distance of around 3 m. In the third measurement setup, the distance between the antenna arrays is about 8 m. The signals are obstructed and scattered by two solid walls and several metallic cupboards in the corridor of the institute to ensure a non-LOS scenario.

#### B. Implementation Aspects

For the MIMO channel sounding measurements regarding the eigenvalue CDFs and the capacity analysis, sequences of orthogonal polyphases are

transmitted repeatedly over all transmit antennas and the estimated channel impulse responses per receive antenna are averaged during a single MASI frame of  $2 \cdot 10^{16}$  samples. The resulting channel matrices are evaluated according to Sec. II-B.

For the adaptive bit error rate measurements, the applied frame structure in [9] is used and consists of multiple OFDM symbols with a FFT length of  $N_C = 512$  before transmitting the payload. Two OFDM symbols are used for synchronization, one is designed for channel estimation and one precoded OFDM symbol is applied for estimating the effective channel having pre-distorted pilot symbols in frequency-domain. This allows for pre-distortion in realistic scenarios with imperfect channel state information at the transmitter (CSIT) [13]. The CSIT is obtained with the reverse link estimate in TDD with the assumption of channel reciprocity. For further parameters the interested reader is referred to [9].

#### IV. MEASUREMENT RESULTS

Fig. 3 shows the measured CDFs of the eigenvalue amplitudes at 2.44 GHz in a  $2 \times 2$  MIMO anechoic chamber scenario with the multiple antenna demonstrator. The results for the antenna array setup exploiting two orthogonal polarizations show an increased second eigenvalue with a shift of the CDF in the order of 45 dB compared to the collinear antenna setup. This indicates that another eigenmode can be exploited more efficiently for multiplexing transmission. The collinear array setup does not offer the same possibility due to the strong LOS component with no additional reflections.

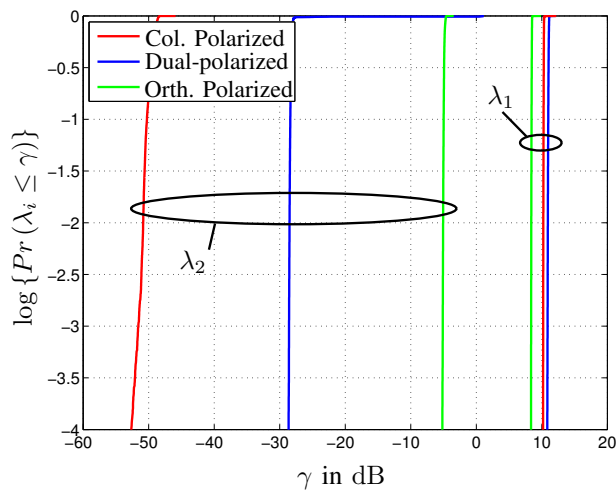


Fig. 3. CDFs of the eigenvalues in the MASI-2  $2 \times 2$ -MIMO system with different antenna array setups in an anechoic chamber

This result also applies to the array setup consisting of two dual-polarized antennas. Similar to collinearly polarized arrays, the dual-polarized antenna arrays have identical polarization characteristics such that no decorrelation of the subchannels is attainable and a small second eigenvalue remains. Nevertheless, on occasion the dual-polarized scheme also offers some improvements in the CDF of the second eigenvalue. This indicates that, although no decoupling is present, it is worth exploiting both polarizations.

In addition, Fig. 4 gives the CDF results for the corridor non-LOS scenario, which indicate a general increase of the eigenvalues for all configurations. However, the slope of the curves is decreased due to the increased scattering outside the anechoic chamber. Interestingly, the performance loss of the collinear arrays is smaller in non-LOS scenarios compared to the orthogonal arrays. Especially the larger eigenvalue of the orthogonally polarized and dual-polarized antennas is decreased. In this case, the application of multiple polarizations does not always pay off and is more interesting in indoor scenarios with strong LOS conditions.

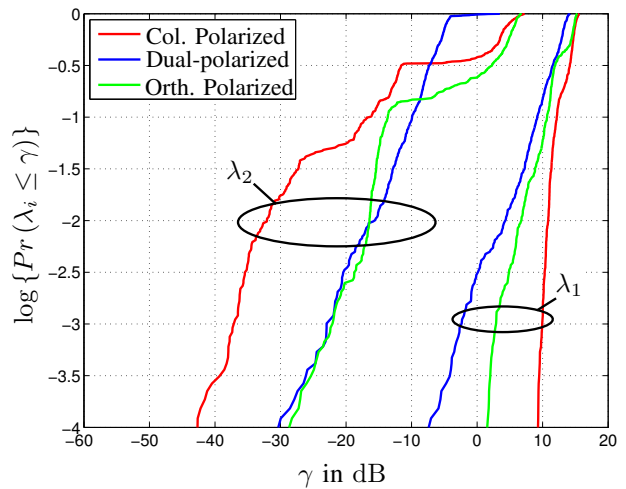


Fig. 4. CDFs of the eigenvalues in the MASI-2  $2 \times 2$ -MIMO system with different antenna array setups in a corridor non-LOS scenario

Regarding the estimated ergodic capacity of the adaptive MIMO scheme, Fig. 5 shows significant gains at high signal-to-noise ratios (SNR), while the gain vanishes at low SNRs. This corresponds to results from information theory, as in low SNR regions beamforming methods should be applied. Therefore, only one single eigenmode is exploited, which was highest for the dual-polarized array results here (cf. Fig. 3). The characteristics of the channels are different for different polarizations. Subsequently, fading cross-correlations between the



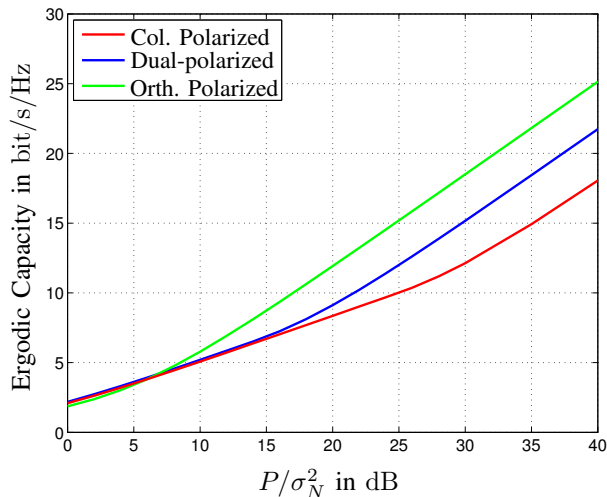


Fig. 5. Estimated ergodic capacity of the MIMO antenna configurations using different polarizations in an anechoic chamber/LOS scenario

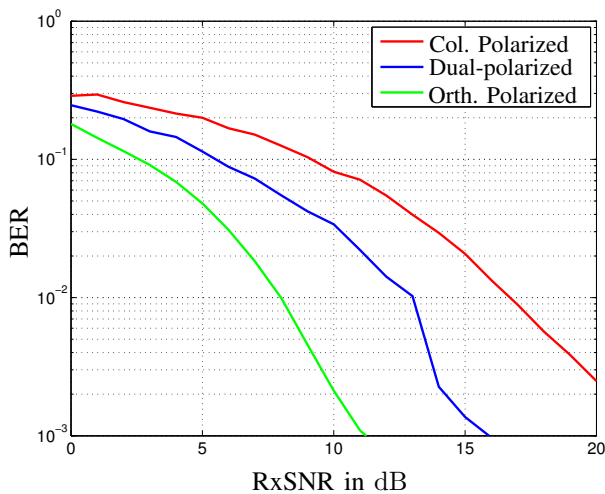


Fig. 6. Bit error rate results for the adaptive MASI-2 MIMO-OFDM system in an office room scenario with a spectral efficiency of  $\eta = 2$  bit/s/Hz

polarizations may even increase the ergodic capacity beyond the case of independent parallel channels.

Now, taking the MASI-2 demonstrator setup of Sec. III-A, Fig. 6 illustrates the bit error rate results for the uncoded adaptive MIMO-OFDM system based on reverse link CSI. Here, a spectral efficiency of  $\eta = 2$  bit/s/Hz is selected for the three investigated antenna array configurations. As already visible in the previous evaluations, the orthogonally polarized antennas provide a larger second eigenvalue, which can be exploited by the bit and power loading algorithm. Consequently, a modulation of lower order is possible on each subcarrier that is used for the data transmission. At the same time, a larger amount of the data, compared to the collinearly polarized antennas, is transmitted on the second eigenmode. This leads to a large BER gain, where the gain of the dual-polarized arrays is smaller compared to the fully decoupled antennas.

## V. CONCLUSION

In this contribution, the application of different antenna setups using dipoles is investigated in terms of polarization. Utilizing orthogonally polarized antennas by using two dipoles, which are oriented perpendicularly to each other, leads to a significantly increased capacity at high SNRs due to the better conditioned channel matrix. Similar observations hold for dual-polarized antenna array elements although no decorrelation of the subchannels is attainable. Measurement results concerning uncoded adaptive MIMO-OFDM systems using bit and power loading that adopt both polarization planes indicate a better BER performance compared to standard collinearly polarized antenna array setups.

## REFERENCES

- [1] G. J. Foschini and M. J. Gans, "On Limits of Wireless Communications in a Fading Environment when using Multiple Antennas," *Wireless Personal Communications*, vol. 6, no. 3, pp. 311–335, Dec. 1998.
- [2] R. U. Nabar, H. Bölcskei, V. Erceg, D. Gesbert, and A. J. Paulraj, "Performance of Multiantenna Signaling Techniques in the Presence of Polarization Diversity," *IEEE Transactions on Signal Processing*, vol. 50, no. 10, pp. 2553–2562, Oct. 2002.
- [3] Y. C. Huang and B. Senadji, "Orientation Invariant Diversity Gain using Transmit Polarization Diversity," in *2nd International Conference on Signal Processing and Communication Systems (ICSPCS)*, Gold Coast, Australia, Dec. 2008.
- [4] R. G. Vaughan, "Polarization diversity in mobile communications," *IEEE Transactions on Vehicular Technology*, vol. 39, no. 3, pp. 177–186, Aug. 1990.
- [5] T. Wirth, V. Jungnickel, A. Forck, S. Wahls, V. Venkatkumar, T. Haustein, and H. Wu, "Polarisation Dependent MIMO Gains on Multiuser Downlink OFDMA with a 3GPP LTE Air Interface in Typical Urban Outdoor Scenarios," in *International ITG Workshop on Smart Antennas (WSA)*, Darmstadt, Germany, Feb. 2008.
- [6] J. A. C. Bingham, "Multicarrier Modulation for Data Transmission: An Idea whose time has come," *IEEE Communications Magazine*, vol. 28, pp. 5–14, May 1990.
- [7] T. Pratt, B. Walkenhorst, and S. Nguyen, "Adaptive Polarization Transmission of OFDM Signals in Channels with Polarization Mode Dispersion and Polarization-dependent Loss," *IEEE Transactions on Wireless Communications*, vol. 8, no. 7, pp. 3354–3359, Jul. 2009.
- [8] C. Waldschmidt, C. Kuhnert, T. Fugen, and W. Wiesbeck, "Measurements and Simulations of Compact MIMO-Systems Based on Polarization Diversity," in *IEEE Topical Conference on Wireless Communication Technology*, Oct. 2003.
- [9] M. Stefer, M. Petermann, M. Schneider, D. Wübben, and K.-D. Kammeyer, "Influence of Non-reciprocal Transceivers at 2.4 GHz in Adaptive MIMO-OFDM Systems," in *14th International OFDM-Workshop (InOWo)*, Hamburg, Germany, Sep. 2009.
- [10] J. P. Kermaol, P. E. Mogensen, S. H. Jensen, J. B. Andersen, F. Frederiksen, T. B. Sorensen, and K. I. Pedersen, "Experimental Investigation of Multipath Richness for Multi-Element Transmit and Receive Antenna Arrays," in *IEEE Vehicular Technology Conference (VTC Spring)*, Tokyo, Japan, May 2000.
- [11] B. S. Krongold, K. Ramchandran, and D. L. Jones, "Computationally efficient optimal power allocation algorithms for multicarrier communication systems," *IEEE Transactions on Communications*, vol. 48, pp. 23–27, Jan. 2000.
- [12] R. G. Gallager, *Information Theory and Reliable Communications*. Wiley, Jan. 1968.
- [13] H. Busche, A. Vanaev, and H. Rohling, "SVD-based MIMO Precoding and Equalization Schemes for Realistic Channel Knowledge: Design Criteria and Performance Evaluation," *Wireless Personal Communications - An International Journal*, vol. 48, no. 3, pp. 347–359, Jun. 2008.